



## RESEARCH ARTICLE

10.1029/2023JA031419

### Key Points:

- Cusp-aligned arcs (CAAs) observed by the Defense Meteorological Satellite Program spacecraft occur frequently for northward interplanetary magnetic field
- Cluster and Geotail observations show that the arcs are accompanied by trapped plasma at high latitudes in the magnetotail
- We interpret CAAs as a signature of a magnetosphere almost entirely closed by dual-lobe reconnection

### Correspondence to:

S. E. Milan,  
[steve.milan@le.ac.uk](mailto:steve.milan@le.ac.uk)

### Citation:




Milan, S. E., Mooney, M. K., Bower, G. E., Taylor, M. G. G. T., Paxton, L. J., Dandouras, I., et al. (2023). The association of cusp-aligned arcs with plasma in the magnetotail implies a closed magnetosphere. *Journal of Geophysical Research: Space Physics*, 128, e2023JA031419. <https://doi.org/10.1029/2023JA031419>

Received 17 FEB 2023  
Accepted 19 JUN 2023

©2023. The Authors.

This is an open access article under the terms of the [Creative Commons Attribution License](https://creativecommons.org/licenses/by/4.0/), which permits use, distribution and reproduction in any medium, provided the original work is properly cited.

# The Association of Cusp-Aligned Arcs With Plasma in the Magnetotail Implies a Closed Magnetosphere

S. E. Milan<sup>1</sup> , M. K. Mooney<sup>1</sup>, G. E. Bower<sup>1</sup> , M. G. G. T. Taylor<sup>2</sup>, L. J. Paxton<sup>3</sup> , I. Dandouras<sup>4</sup> , A. N. Fazakerley<sup>5</sup>, C. M. Carr<sup>6</sup> , B. J. Anderson<sup>7</sup> , and S. K. Vines<sup>7</sup> 

<sup>1</sup>School of Physics and Astronomy, University of Leicester, Leicester, UK, <sup>2</sup>ESA/ESTEC, Noordwijk, The Netherlands,

<sup>3</sup>William B. Hanson Center for Space Sciences, University of Texas at Dallas, Richardson, TX, USA, <sup>4</sup>Institut de Recherche en Astrophysique et Planétologie (IRAP), CNRS, Université Paul Sabatier, Toulouse, France, <sup>5</sup>Mullard Space Science Laboratory, University College, London, UK, <sup>6</sup>Imperial College, London, UK, <sup>7</sup>Applied Physics Laboratory, Johns Hopkins University, Laurel, MD, USA

**Abstract** We investigate a 15-day period in October 2011. Auroral observations by the Special Sensor Ultraviolet Spectrographic Imager instrument onboard the Defense Meteorological Satellite Program F16, F17, and F18 spacecraft indicate that the polar regions were covered by weak cusp-aligned arc (CAA) emissions whenever the interplanetary magnetic field (IMF) clock angle was small,  $|\theta| < 45^\circ$ , which amounted to 30% of the time. Simultaneous observations of ions and electrons in the tail by the Cluster C4 and Geotail spacecraft showed that during these intervals dense ( $\approx 1 \text{ cm}^{-3}$ ) plasma was observed, even as far from the equatorial plane of the tail as  $|Z_{\text{GSE}}| \approx 13 R_E$ . The ions had a pitch angle distribution peaking parallel and antiparallel to the magnetic field and the electrons had pitch angles that peaked perpendicular to the field. We interpret the counter-streaming ions and double loss-cone electrons as evidence that the plasma was trapped on closed field lines, and acted as a source for the CAA emission across the polar regions. This suggests that the magnetosphere was almost entirely closed during these periods. We further argue that the closure occurred as a consequence of dual-lobe reconnection. Our finding forces a significant re-evaluation of the magnetic topology of the magnetosphere during periods of northwards IMF.

**Plain Language Summary** The magnetosphere is usually assumed to contain both open and closed magnetic flux. Closed magnetic field lines have both ends connected to the Earth; open field lines connect to the Earth at one end and into the interplanetary medium at the other. There tends to be little plasma on open field lines as the particles escape down the magnetotail, whereas plasma on closed field lines is trapped. Open flux near the poles naturally explains the oval configuration of Earth's auroras, with a lack of auroras at very high latitudes where there is no plasma to cause emissions. Somewhat unexpectedly, we show that auroral emission near the poles is common and that at these times there is significant plasma in the magnetotail, indicating that the magnetosphere contains only closed flux. We propose that this magnetic configuration is formed by a process known as dual-lobe magnetic reconnection which occurs when the interplanetary magnetic field (IMF) within the solar wind points northwards. We must re-evaluate the standard picture of magnetospheric structure during these periods of northwards IMF.

## 1. Introduction

In this study we investigate repeated occurrences of cusp-aligned arcs (CAAs), the poorly understood situation in which weak auroral emissions fill the polar regions, during a 15-day interval in 2011. We conclude that CAAs are a common occurrence during periods of northward interplanetary magnetic field (IMF), and that they are a signature of a nearly- or entirely-closed magnetosphere. This forces a significant re-evaluation of the magnetic topology of the magnetosphere during northward IMF.

The coupling between the solar wind and the magnetosphere is relatively well understood for southward-directed IMF: as first proposed by Dungey (1961), magnetic reconnection near the subsolar magnetopause opens previously-closed magnetic flux which then forms the magnetotail lobes; thereafter, magnetic reconnection in the central plane of the tail recloses flux which returns to the dayside, resulting in the Dungey cycle of magnetospheric convection. The northern and southern ionospheric polar caps, the dim regions encircled by the auroral ovals, are the ionospheric projection of the open flux forming the lobes, and their size can be used to quantify the open flux content of the magnetosphere,  $F_{\text{PC}}$  (e.g., Milan et al., 2003). This naturally explains many aspects

of magnetospheric structure and dynamics, including the formation of the magnetotail, the twin-cell ionospheric convection pattern, the morphology of the auroral oval, the plasma populations within the magnetosphere, and the evacuated magnetotail lobes. When time-varying magnetic reconnection rates are considered, the expanding/contracting nature of the polar cap and the substorm cycle can be understood (Cowley & Lockwood, 1992; Lockwood & Cowley, 1992; Milan et al., 2021; Siscoe & Huang, 1985). Typically,  $F_{PC}$  varies between 0.3 and 0.9 GWb (Milan et al., 2003, 2007). However, it can become as low as 0.2 GWb ( $\sim 2.5\%$  of the 8 GWb associated with the terrestrial dipole) during particularly extreme nightside reconnection events, accompanied by a near-total in-filling of the polar regions by bright auroral emission (e.g., Milan et al., 2004). In this paper we show that in fact the polar cap closes entirely, frequently, and with much less fanfare, during periods of northwards IMF.

The coupling during northward-directed IMF is still poorly understood. Although Dungey (1963) correctly proposed that magnetic reconnection would take place at the high latitude magnetopause, tailwards of the cusps, the ramifications are still not fully resolved. The list of northward-IMF (IMF  $B_z > 0$  or NBZ) phenomena includes: single- and dual-lobe reconnection (e.g., Cowley, 1981; Fuselier et al., 2012), reverse convection in the polar cap (e.g., Huang et al., 2000; Reiff & Burch, 1985), NBZ field-aligned currents poleward of the noon auroral oval (e.g., Iijima et al., 1984), cusp auroral spots (e.g., Carter et al., 2018, 2020; Frey, 2007; Frey et al., 2002; Milan et al., 2000), transpolar or polar cap arcs (e.g., Cumnock et al., 2002; Fear et al., 2014; Frank et al., 1982; Kullen et al., 2002; Milan et al., 2005), horse-collar auroras (HCAs) (e.g., Bower, Milan, Paxton, & Anderson, 2022; Hones Jr et al., 1989; Milan, Carter, Bower, et al., 2020), CAAs (e.g., Milan et al., 2022; Wang et al., 2023; Y. Zhang et al., 2016; Q.-H. Zhang et al., 2020), the NBZ low-latitude boundary layer and the cold, dense plasma sheet (e.g., Fujimoto et al., 1998, 2000; Imber et al., 2006; Øieroset et al., 2005, 2008; Terasawa et al., 1997). More information can be found in recent reviews of NBZ phenomena by Fear (2021) and Hosokawa et al. (2020).

A key question regarding periods of NBZ is the degree to which the magnetosphere loses open magnetic flux, the resulting distribution of open and closed flux in the polar regions and magnetotail, and the relation to high latitude auroral features. A number of simulations have suggested that during prolonged NBZ the magnetosphere can become completely closed (e.g., Siscoe et al., 2011; Song et al., 1999), and observations of trapped plasma in regions of the magnetosphere that are normally open (e.g., Øieroset et al., 2008) support this possibility. It has also been argued that there are periods when the polar regions fill with auroral emissions and that this is the signature of a closed magnetosphere (e.g., Y. Zhang et al., 2009; Milan et al., 2022). In this study we link these two pieces of evidence—trapped plasma in the magnetotail and auroral emissions at high latitudes—to provide strong evidence that the magnetosphere does indeed close.

It has been suggested that polar cap arcs—a catch-all term for high latitude auroral phenomena which tend to be elongated in a sun-aligned or cusp-aligned direction—can come in different varieties which may be associated with either open or closed magnetic flux (e.g., Bower, Milan, Paxton, & Imber, 2022; Carlson & Cowley, 2005; Reidy et al., 2020). Evidence suggests that the most prominent of polar cap arcs, those also known as transpolar arcs or theta auroras, are likely associated with closed magnetic flux (Coxon et al., 2021; Fear et al., 2014; Fryer et al., 2021), proposed to be produced by magnetic reconnection in the magnetotail (Fear & Milan, 2012a, 2012b; Milan et al., 2005). Closed magnetic flux traps plasma in the magnetotail which then acts as a source for auroral precipitation.

Weaker polar cap auroras often appear as multiple arcs which fan out from the cusp region, termed CAAs by Y. Zhang et al. (2016). These features have received less attention than the more prominent transpolar arcs as the emissions tend to be so weak that they were not regularly observed by global auroral imaging missions such as Polar or IMAGE. Rather, they are better observed from the ground (e.g., Hosokawa et al., 2011; Ismail et al., 1977) or from low altitude auroral cameras such as the Special Sensor Ultraviolet Spectrographic Imager (SSUSI) (Paxton et al., 1992) onboard the Defense Meteorological Satellite Program (DMSP) spacecraft. This results in observations with only limited geographical coverage and/or temporal cadence, which hampers an understanding of their dynamics. The question remains: do CAAs form on closed field lines or the open flux of the largely-evacuated magnetotail lobes, and if the latter then what is the source of the auroral precipitation?

During prolonged NBZ, the polar cap can contract and become teardrop-shaped, leading to the formation of the HCAs configuration (Hones Jr et al., 1989). Bower, Milan, Paxton, and Anderson (2022) and Milan, Carter, Bower, et al. (2020) suggested that this is caused by the closure of magnetic flux by dual-lobe reconnection (DLR) occurring during periods of near-zero IMF clock angle, a suggestion recently supported by numerical simulations (Wang et al., 2023). Milan et al. (2022) went on to propose that if DLR continues until (almost) all

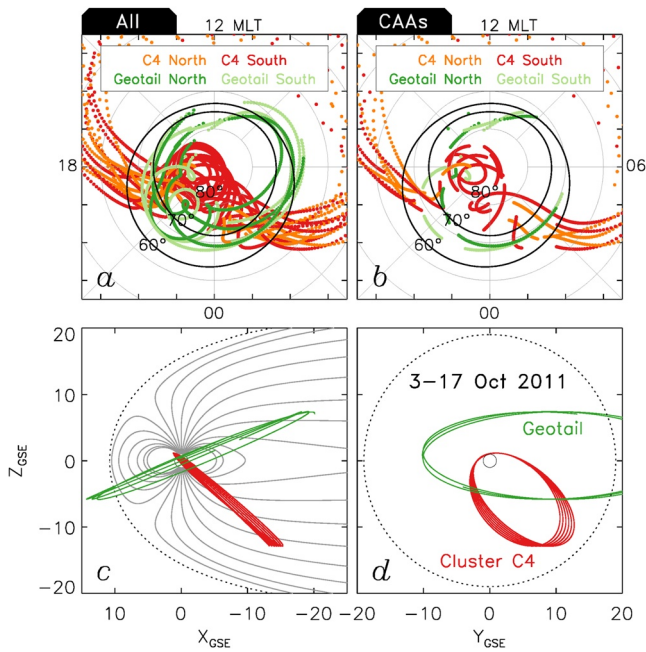


**Figure 1.** (a) Polar projection of field-line tracings from the location of Cluster and Geotail to the northern (orange and dark green) and southern (red and light green) hemisphere ionospheres for the period 3–17 October 2011, using the T96 model with input parameters for  $P_{\text{dyn}} = 2$  nPa,  $D_{\text{st}} = -10$  nT,  $B_y = 0$  and  $B_z = 5$  nT. An average auroral oval for  $K_p = 1$  is overlaid for reference. (b) The same as panel (a), except for periods when cusp-aligned arcs are observed (see text for details). (c) The orbit of Cluster C4 (red) and Geotail (green) for the period of study, in the Geocentric Solar Ecliptic (GSE)  $X - Z$  plane. The T96 magnetic field configuration at 13 UT on 7 October 2011 (DOY 280) is superimposed in gray. (d) The orbit of Cluster and Geotail for the period of study, in the GSE  $Y - Z$  plane; the location of the magnetopause at  $X = -10 R_E$  is shown for reference.

of the open magnetospheric flux is closed, then the polar cap disappears and the polar regions can become filled with cusp-aligned auroral arcs (CAAs). It is this auroral scenario—HCAs followed by CAAs—that we focus on in this paper: we argue that these features are indeed associated with closed magnetic flux.

Dual-lobe reconnection should be an efficient mechanism by which the magnetosphere can capture solar wind plasma (e.g., Imber et al., 2006), and it has been proposed that over time this can lead to the formation of a cold, dense plasma sheet (Øieroset et al., 2005, 2008). However, this is not the only means by which solar wind plasma is thought to enter the magnetosphere during periods of NBZ, with inward diffusion at the magnetotail flanks (Fujimoto et al., 1998, 2000; Hasegawa et al., 2004; Taylor et al., 2008; Terasawa et al., 1997) or direct entry onto open field lines through (single) lobe reconnection (Bogdanova et al., 2008; Mailyan et al., 2015; Shi et al., 2013) being other commonly discussed mechanisms. It is unclear, however, how efficient diffusion can be, how quickly captured solar wind plasma can be redistributed throughout the magnetosphere, and why the plasma remains near the Earth and does not escape back to the solar wind down the open field lines of the lobes, as it does for southwards IMF. The timescales on which plasma gains entry to the tail and the magnetic topology on which it resides, are then key questions that must also be addressed.

Carlson and Cowley (2005) proposed that if polar cap arcs do form on open field lines, then polar rain could be a sufficient source of plasma if accelerated downwards by flow shears in the ionospheric convection. This then poses the question as to how such flow shears are produced. Recently, Wang et al. (2023) and Q.-H. Zhang et al. (2020) suggested that the shears are introduced into the magnetosphere by Kelvin-Helmholtz surface waves excited on the magnetotail flanks by the flow of the solar wind. However, this does not resolve the source of the precipitating plasma. On the other hand, Milan et al. (2022) proposed that DLR could close the magnetosphere, trapping plasma to act as a reservoir for auroral phenomena, and that continuing reconnection between the IMF and the now-closed magnetosphere would

drive the magnetosphere in reverse convection (Siscoe et al., 2011). In this situation, “lobe reconnection” would be something of a misnomer, but we hesitate to introduce new terminology. In this scenario, the closed magnetosphere will be filled with trapped solar wind plasma and, according to Milan et al. (2022), flow shears produced by lobe reconnection can then accelerate this trapped plasma into the atmosphere to form the CAAs. Whereas Carlson and Cowley (2005) suggested that the source of plasma to produce weak polar cap arcs was polar rain on open field lines, instead Milan et al. (2022) proposed that the source is solar wind plasma captured by DLR and trapped on closed field lines.

In this study we examine plasma populations observed in the near-Earth tail by the C4 spacecraft of the Cluster constellation (Escoubet et al., 2001) and the Geotail (Nishida, 1994) spacecraft during a prolonged period in October 2011 when auroral observations from F16, F17, and F18 of the Defense Meteorological Spacecraft Program detected multiple instances of CAAs. Dense plasma is repeatedly found in regions that would normally be occupied by the evacuated open field lines of the northern and southern lobes, and it is concluded that the magnetosphere is almost entirely closed and the plasma is trapped, providing a source for the high latitude auroral emission.

## 2. Observations

The period under investigation is the 3–17 October 2011 (days-of-year 276–290), which encompasses six orbits of the Cluster constellation during its tail season and three orbits of Geotail; the orbits are shown in Figure 1. At this time, the orbit of C4 was inclined such that it was southwards of the neutral sheet for most of the time, except near perigee. During the study interval, C4 reached  $Z_{\text{GSE}} \approx -13 R_E$ ,  $X_{\text{GSE}} \approx -14 R_E$  at apogee, and it was

located relatively centrally in the tail,  $0 < Y_{\text{GSE}} < 10 R_E$  in the first half of each orbit, but closer to the dusk flank in the second. The orbit of Geotail was such that it sampled the magnetotail northwards of the neutral sheet, up to  $Z_{\text{GSE}} \approx 8 R_E$  at  $X_{\text{GSE}} \approx -19 R_E$ . A representative magnetic field tracing in the T96 model (Tsyganenko, 1995), with input parameters  $P_{\text{dyn}} = 2 \text{ nT}$ ,  $D_{\text{st}} = -10 \text{ nT}$ , and IMF  $B_y = 0$  and  $B_z = 5 \text{ nT}$ , is overlaid for reference. These parameters were chosen to represent a quiet NBZ magnetosphere, and will be used throughout the rest of the study to compare with magnetic field observations. As the plasma sheet is usually confined to  $|Z| < 5 R_E$ , for much of their orbits Geotail and C4 are expected to be within the northern and southern lobes of the magnetotail, respectively. Field line tracings from the locations of the two spacecraft to the northern and southern ionospheres are also presented in panel c, with a  $K_p = 1$  average auroral oval superimposed for reference. This indicates that near apogee C4 would normally be expected to map to the central polar cap in the southern hemisphere, and that Geotail would frequently map to the nightside polar cap in the northern hemisphere.

Auroral observations during this period are provided by the Special Sensor Ultraviolet Spectrographic Imager or SSUSI experiment (Paxton et al., 1992) onboard Defense Meteorological Satellite Program spacecraft DMSP-F16, -F17, and -F18. The DMSP spacecraft have sun-synchronous orbits near an altitude of 850 km. SSUSI measured auroral luminosity in a swath either side of the spacecraft orbit in the Lyman–Birge–Hopfield short (LBHs) band, 140–150 nm (see Paxton and Zhang, 2016; Paxton et al., 2017, 2021 and the references cited therein for further description of the instrument and data products). Measurements of the distribution of magnetosphere-ionosphere field aligned currents (FACs) were provided by the Active Magnetosphere and Planetary Electrodynamics Response Experiment (AMPERE) technique (Anderson et al., 2000; Coxon et al., 2018; Waters et al., 2001). We also make use of ionospheric flow observations provided by the Super Dual Auroral Radar Network (SuperDARN; Chisham et al., 2007) and the Ion Driftmeter (IDM) component of the Special Sensors–Ions, Electrons, and Scintillation thermal plasma analysis package or SSIES instrument (Rich & Hairston, 1994) onboard the DMSP spacecraft. Solar wind parameters were taken from the OMNI data set (King & Papitashvili, 2005).

Figure 2 shows 12 snapshots of the auroral morphology from DOYs 278 to 280. Below this, a keogram of the observations along the dawn–dusk meridian made by DMSP-F16/SSUSI in the northern hemisphere is shown, along with the IMF clock angle from OMNI. Around 10:20 UT on DOY 278 (panels a and b), the IMF had a southwards component and typical twin-cell ionospheric flows were observed by SuperDARN and DMSP/IDM (not shown for brevity). The auroral morphology was also typical, showing an oval surrounding a dim polar cap, with evidence for substorm activity on the nightside. Between approximately 16:00 UT, DOY 278, and 13:00 UT, DOY 279, the IMF turned northwards. During this period the auroras dimmed, contracted to higher latitudes and acquired a horse-collar auroral configuration, before the polar regions filled with weak auroral emission mainly in the form of CAAs (c–f). CAAs are seen in both northern and southern hemispheres, panels c and e being from the north and d and f being from the south. Then the IMF turned southwards again, twin-cell convection resumed, and the polar cap reopened (g and h). There followed another period of NBZ, during which CAAs reformed (i and j), before again a southward turning and a reopening of the polar cap (k–l). The lower panels clearly show the expansions and contractions of the auroral oval with changes in clock angle, and the presence of auroral emissions at high latitudes during periods when the clock angle is near zero,  $|\theta| < 45^\circ$ , highlighted in red.

Over the rest of the period considered several other intervals of CAAs were found, as will be indicated in later figures by horizontal red bars. The start and end times of these intervals are approximate due to the relatively coarse cadence of the DMSP orbits; there are also periods when it was not possible to positively identify whether CAAs were present or not, due to only partial coverage of the polar regions by the SSUSI field-of-view. During periods when HCAs or CAAs were present, the ionospheric flows measured by SuperDARN and DMSP/IDM and the field-aligned currents observed by AMPERE were consistent with the observations reported by Milan, Carter, Bower, et al. (2020) and Milan et al. (2022)—reverse lobe convection, NBZ FACs at noon—suggesting that DLR was responsible for closing the magnetosphere. The occurrence of CAAs when  $|\theta| < 45^\circ$  is also consistent with the statistical occurrence of HCAs (Bower, Milan, Paxton, & Anderson, 2022), thought to be the auroral precursor to CAAs.

In Figure 3 we present the patterns of precipitating particles observed by the Special Sensor for Precipitating Particles version 4 or SSJ/4 instrument (Hardy, 1984) onboard DMSP-F17 during the passes shown in Figure 2 panels f and g. The first is from a period when CAAs were observed by DMSP-F17/SSUSI, the second when the polar cap appeared open. Although the CAAs in panel f are very faint, the corresponding spectrograms in Figure 3 (left panels) show inverted-V electron signatures across the polar regions, with patches of ion precipitation as

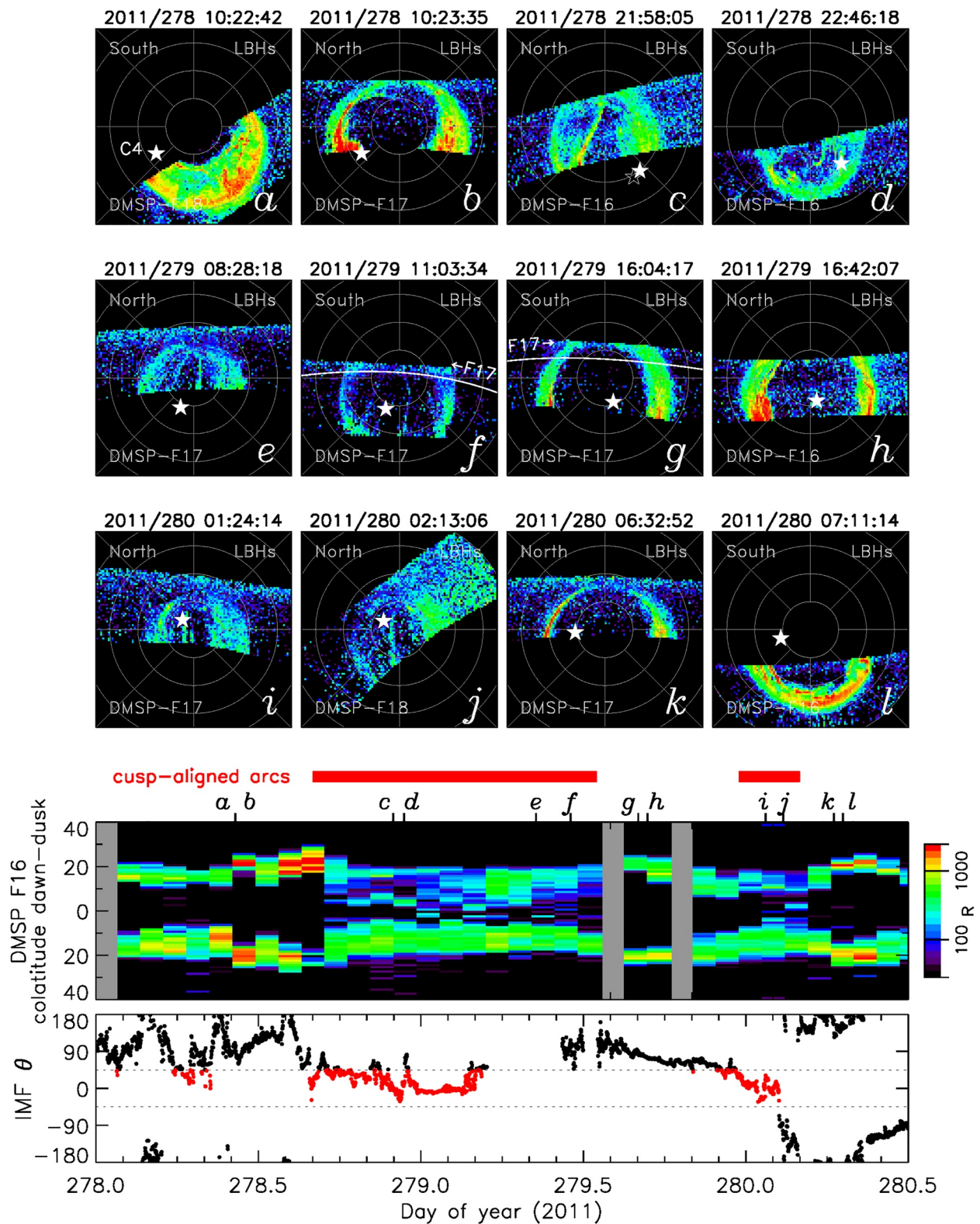
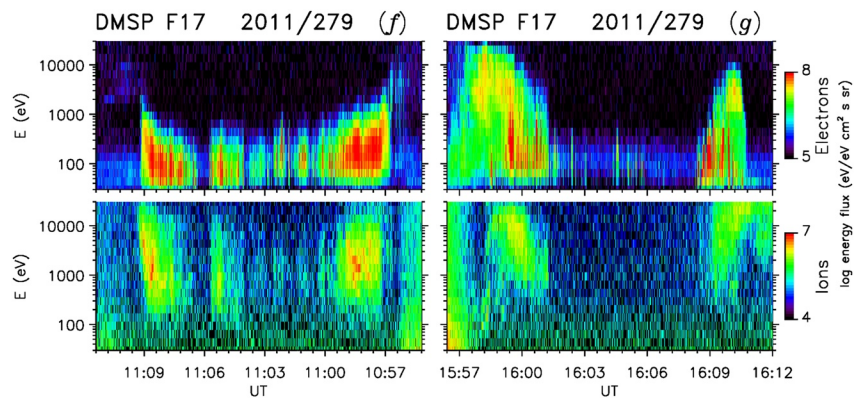


Figure 2.



**Figure 3.** Spectrograms of precipitating electrons and ions measured by the SSJ/4 instrument from two passes of DMSP-F17, corresponding to panels (f) and (g) of Figure 2. The time axis of the left-hand spectrogram is reversed so dusk is to the left and dawn to the right in both cases.

well, consistent with the observations of Milan et al. (2022) and Q.-H. Zhang et al. (2020) (Note that the time axis is reversed for these spectrograms, such that dusk is to the left and dawn to the right.). By contrast, the right panels of Figure 3 show the regions polewards of the main auroral oval are largely devoid of plasma, indicative of an open polar cap. We will later argue that the magnetosphere is (almost) entirely closed during the overpass of panel f, in which case we might expect continuous precipitation across the polar regions; as discussed below, we expect that the inverted-V and patchy ion precipitation is associated with shears in the ionospheric convection pattern which accelerate otherwise-trapped plasma to produce cusp-aligned auroral arcs.

We use Cluster C4 observations from the Composition and Distribution Function analyzer of the Cluster Ion Spectrometry instrument (C4/CIS-CODIF; Rème et al., 1997), the Plasma Electron And Current Experiment (C4/PEACE; Johnstone et al., 1997), and the Fluxgate Magnetometer (C4/FGM; Balogh et al., 1997). Figure 4 covers the period 3–9 October, spanning the first three C4 orbits considered and encompassing the interval shown in Figure 2. The panels are presented in the following order. (a) The Geocentric Solar Ecliptic (GSE)  $X$ ,  $Y$ , and  $Z$  ( $R_E$ ) position of C4. (b) The  $B_x$ ,  $B_y$ ,  $B_z$  components of the magnetic field measured by C4/FGM in GSE coordinates. Dots indicate predications of the magnetic field measurements by the T96 (Tsyganenko, 1995) model, with fixed inputs (as before). (c) The proton density,  $n_p$ , observed by C4/CIS-CODIF. Horizontal red bars indicate when CAAs were observed by DMSP/SSUSI. (d) The proton differential energy flux spectrogram measured by C4/CIS-CODIF. (e) The electron differential energy flux spectrogram measured by C4/PEACE. (f) A dawn-dusk keogram of auroral emissions observed by DMSP-F16/SSUSI in the northern hemisphere. (g) A dawn-dusk keogram of FAC density measured by AMPERE in the northern hemisphere, with red/blue indicating up/down currents. (h) The clock angle of the IMF,  $\theta$ , highlighted in red when  $|\theta| < 45^\circ$ . (i) The Geocentric Solar Magnetic  $B_x$ ,  $B_y$ ,  $B_z$  components of the IMF from OMNI. (j) The solar wind speed and density from OMNI.

The SSUSI keogram (f) reveals that at most times there was little auroral emission inside the auroral oval, consistent with an open polar cap, except at the times of CAAs (red bars in c) when  $|\theta| < 45^\circ$ . The region 1 and 2 (R1/R2) FACs (Iijima & Potemra, 1976) observed by AMPERE (g) were enhanced when the polar cap was open, indicating Dungey cycle driving of the magnetosphere by subsolar reconnection, especially during periods with IMF  $B_z < 0$  nT,  $|\theta| > 90^\circ$ . When CAAs were present the R1/R2 FACs were weak, though NBZ FACs tended to be observed at noon (not shown).

Near the perigee of each orbit (marked PG) when  $|Z| < 5 R_E$ , C4 passed through the plasma sheet and ring current regions and enhanced proton densities,  $n_p$ , were observed (c). During the first orbit of Figure 4 almost no plasma was observed when  $Z < -5 R_E$ , consistent with the open lobe. In contrast, while C4 was near perigee on DOY

**Figure 2.** Snapshots of the LBHs auroral configuration in the northern and southern hemispheres observed by DMSP/SSUSI onboard DMSP-F16, -F17, and -F18 between 5 and 7 October 2011. Each panel is presented in a geomagnetic latitude and local time format, with noon toward the top and dawn toward the right. Gray circles indicate geomagnetic latitude in steps of  $10^\circ$ . Filled and unfilled stars indicate the ionospheric footprints of Cluster C4 in the southern and northern hemispheres, respectively. White lines in panels (f) and (g) show the DMSP spacecraft track. Of the two lower panels, the top one shows a keogram of auroral emissions observed by DMSP-F16/SSUSI along the dawn-dusk meridian of the northern hemisphere; gray vertical bars indicate where data is missing. Red horizontal bars indicate the times that cusp-aligned arcs were observed. The bottom panel is clock angle, highlighted in red when  $|\theta| < 45^\circ$ .

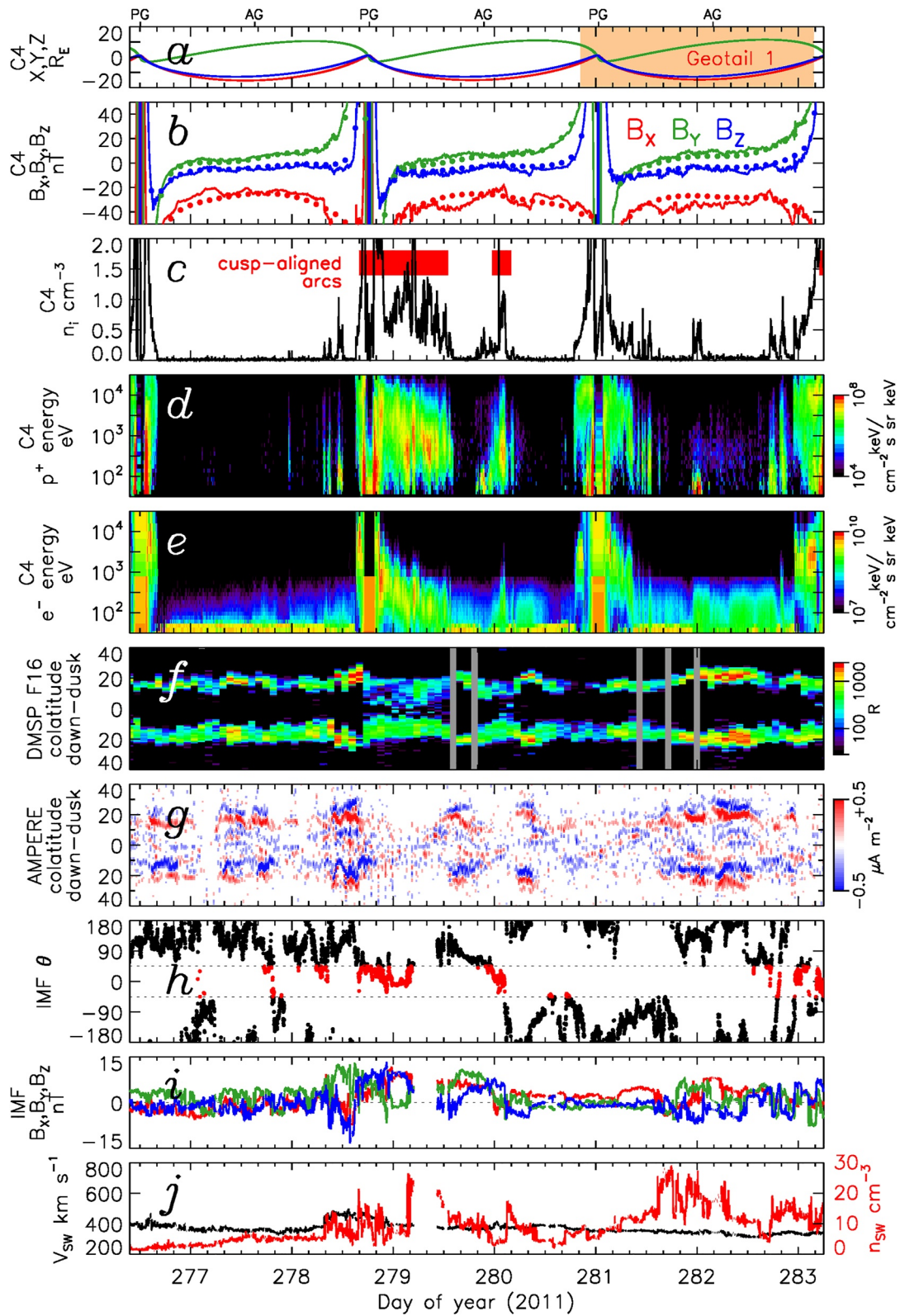


Figure 4.

278 the IMF turned northwards and CAAs were observed, and throughout this period C4 was engulfed in protons with  $n_i \approx 1 \text{ cm}^{-3}$  up to near apogee (AG) on DOY 279. As the IMF turned southwards around 13:00 UT on DOY 279, the density returned to typical lobe values,  $n_i < 0.1 \text{ cm}^{-3}$ . Around 00 UT on DOY 280 CAAs were once again observed, and  $n_i$  rose to near  $1 \text{ cm}^{-3}$ , only to drop again at 04 UT as the IMF turned southwards; the IMF remained predominantly southwards for the duration of the third orbit, and  $n_i$  remained low throughout (except for a short period near apogee, see below).

The C4/CIS-CODIF spectrogram (d) indicates that the CAA-related ions had energies between several 100s and several 1000s eV. (We note that at the apogees of the second and third orbits a brief interval of cold,  $<100 \text{ eV}$ , ions was also observed.) The C4/PEACE spectrogram (e) indicates that the ions were accompanied by electrons, with energies below about 1 keV. In the first CAA interval of DOY 279 the ions, and especially the electrons, reduced in energy with time, indicating a cooling of the plasma, though it is unclear if this was a temporal or spatial effect.

Figure 5 presents the next three orbits of C4. During this period, the IMF  $|\theta| < 45^\circ$  for much of the time, and there were several intervals of CAAs observed by DMSP/SSUSI. Accompanying these intervals, C4/CIS-CODIF saw elevated  $n_i$ , where otherwise lobe conditions might have been expected. During DOYs 287–290, there were repeated swings between  $|\theta| < 45^\circ$  and  $|\theta| > 45^\circ$ , and CAAs and protons came and went in tandem.

Figure 6 focusses on the two intervals of CAAs presented in Figures 2 and 4. In addition to the spectrograms, pitch angle distributions of the ions (d) and electrons (f) are shown. The proton pitch angle fluxes are integrated across the full energy range of the CIS-CODIF instrument; the electron fluxes are calculated from the low energy electron analyzer head of the PEACE instrument, limited to energies above 100 eV to remove the contribution of photoelectrons. During periods of CAAs, and when C4 was not too close to the Earth, ion pitch angles were concentrated at  $0^\circ$  and  $180^\circ$ , indicating two counter-streaming populations. The electron pitch angles, conversely, peaked at  $90^\circ$ , with a distinct lack of electrons near  $0^\circ$  and  $180^\circ$ , indicating a double loss-cone distribution. The double loss-cone electron distribution is similar to that observed by Fear et al. (2014) above a transpolar arc, and is indicative of plasma trapped on closed field lines. The counter-streaming ions support this conclusion that the field is closed. We note that the ion and electron densities during the periods of CAAs were quite variable: although the trapped plasma was not uniformly distributed, it was present continuously until 12 UT, DOY 279. The solar wind density was variable during this period, but it is not clear if variations in ion/electron density and energy observed by C4 are correlated with enhancements in  $n_{sw}$ . As noted previously, the ion and electron energies decreased overall with time, which might indicate the progressive mixing of plasma sheet and solar wind populations, leading to the formation of a cold, dense plasma sheet (e.g., Øieroset et al., 2005).

Just prior to the second period of CAAs, CIS-CODIF detected a beam of low energy ions observed only near  $0^\circ$  pitch angles (i.e., flowing tailward). A similar beam was observed around 00 UT near apogee on DOY 282 (see Figure 4). As there are no counter-streaming ions, we suggest that at these are the signature of plasma escaping to the solar wind along open field lines.

Superimposed on the C4/FGM observations (a) is a model prediction from T96 for fixed NBZ input parameters (as before). There is qualitative agreement between the model and the observations, but during the periods of CAAs the magnitude of the  $B_x$  component was reduced by  $\approx 10 \text{ nT}$  over the periods when CAAs were not present, indicating that the tail was less inflated at these times. This also supports the conclusion that the magnetotail open flux was significantly reduced when CAAs were observed.

Figure 7 presents two time intervals when Geotail was located in the magnetotail; Figures 4 and 5 show that these roughly correspond to orbits 3 and 5 of C4. Panels a and b show that in each case Geotail entered the dusk flank of the magnetotail at the start of the interval, near  $Z \approx 5 R_E$ , and rose to  $Z \approx 8 R_E$  at  $X \approx -19 R_E$ ,  $Y \approx 0 R_E$ . It later exited the dayside magnetopause in the pre-noon sector. Panels e–l present ion and electron spectrograms from the Low Energy Particle (LEP) instrument (Mukai et al., 1994), showing fluxes in the sunward and tailward

**Figure 4.** Observations from 3–10 October 2011, which encompasses three orbits by Cluster. (a) The Geocentric Solar Ecliptic position of C4. Apogees and perigees of the orbit are indicated by AG and PG. Orange highlighting indicates the time of the first Geotail orbit shown in Figure 7. (b) C4/FGM observations of the magnetic field. T96 model predictions for fixed input parameters are indicated as dots. (c) C4/CIS-CODIF ion density measurements. Red bars indicate periods of observation of cusp-aligned arcs by DMSP/SSUSI. (d) C4/CIS-CODIF ion spectrogram. (e) C4/PEACE electron spectrogram. (f) A dawn-dusk keogram of auroral observations by DMSP-F16/SSUSI in the northern hemisphere. (g) A dawn-dusk keogram of field-aligned currents measured by Active Magnetosphere and Planetary Electrodynamics Response Experiment, red and blue being upward and downward field aligned currents, respectively. (h) The clock angle of the interplanetary magnetic field (IMF) from OMNI. The clock angle is highlighted in red when  $|\theta| < 45^\circ$ . (i) The components of the IMF from OMNI. (j) The solar wind speed and density from OMNI.



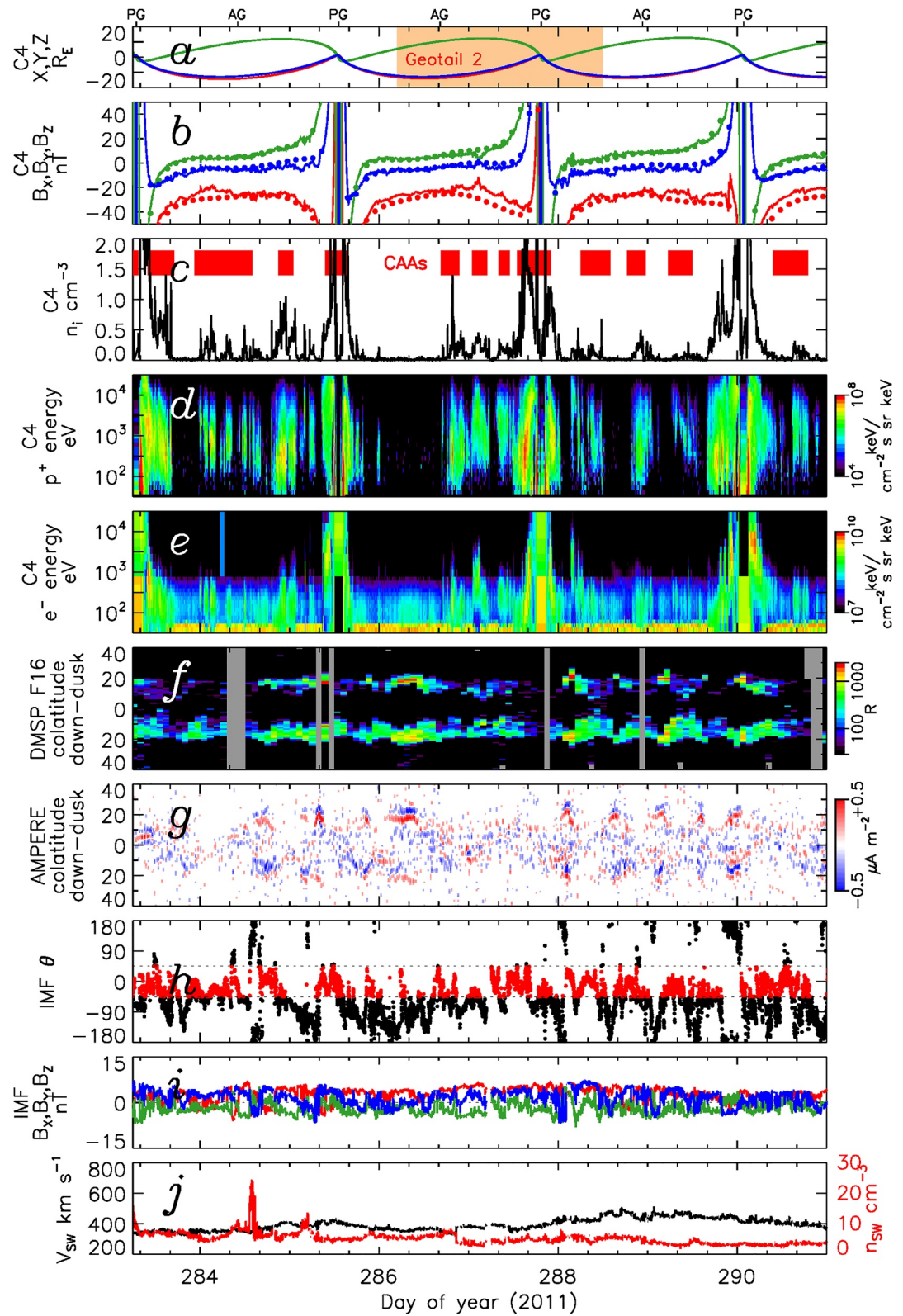
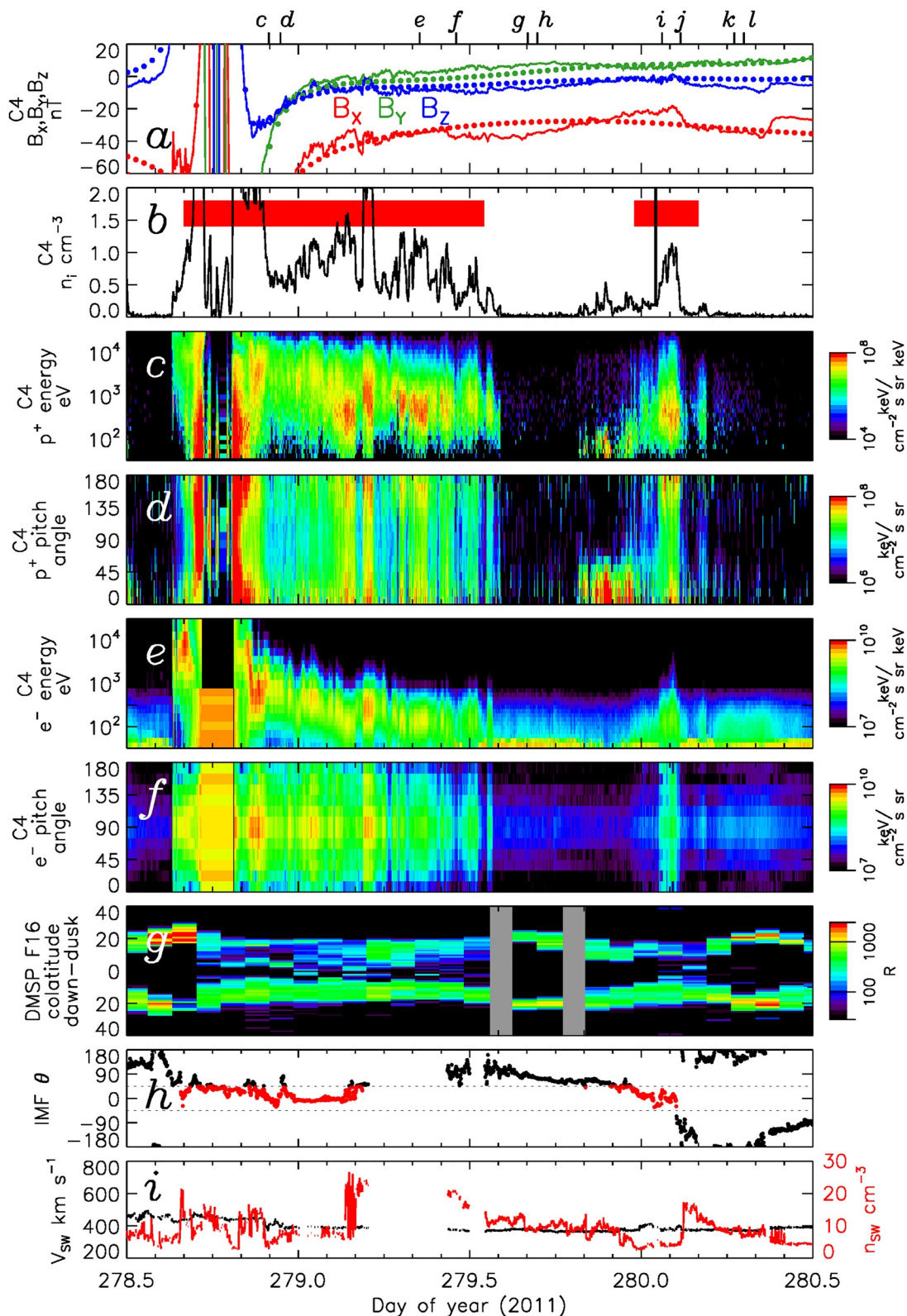
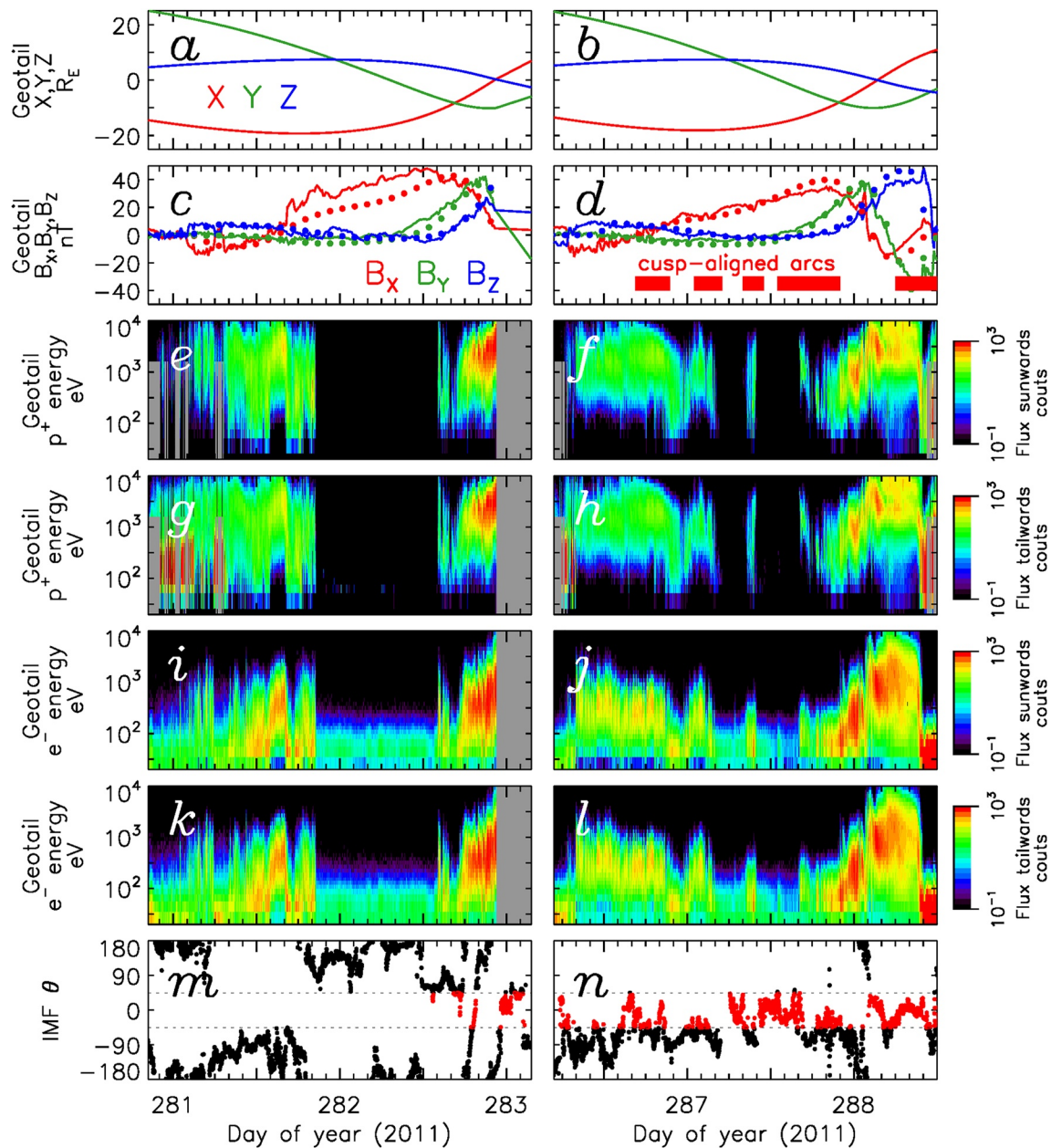


Figure 5. Observations from 10 to 17 October, presented in the same format as Figure 4.



**Figure 6.** Observations from 5–7 October 2011. (a) C4/FGM observations of the magnetic field. T96 model predictions for fixed input parameters are indicated as dots. Letters correspond to panels of Figure 2. (b) C4/CIS-CODIF ion density measurements. Red bars indicate periods of observation of cusp-aligned arcs by DMSP/SSUSI. (c, d) C4/CIS-CODIF ion spectrogram and pitch angle distribution. (e, f) C4/PEACE spectrogram and pitch angle distribution. (g) A dawn-dusk keogram of auroral observations by DMSP-F16/SSUSI. (h) The clock angle of the interplanetary magnetic field from OMNI. The clock angle is highlighted in red when  $|\theta| < 45^\circ$ . (i) The solar wind speed and density from OMNI.



**Figure 7.** Two time periods during which Geotail was located within the magnetotail. (a, b) The Geocentric Solar Ecliptic location of Geotail. (c, d) The magnetic field components measured by Magnetic Field Experiment, with a T96 prediction superimposed. Red bars indicate when cusp-aligned arcs were observed by DMSP/SSUSI. (e, f) Ion spectrograms of fluxes in the sunwards direction. (g, h) Ion spectrograms of fluxes in the tailwards direction. (i, j) Electron spectrograms of fluxes in the sunwards direction. (k, l) Electron spectrograms of fluxes in the tailwards direction. (m, n) interplanetary magnetic field clock angle, highlighted in red when  $|\theta| < 45^\circ$ .

directions. During the first orbit, the plasma sheet was seen as the spacecraft entered and exited the magnetosphere, but the evacuated lobe was encountered from 16 UT on DOY 281 to 14 UT on DOY 282. During this period, IMF  $|\theta| > 45^\circ$  at all times (m). During the second orbit, the plasma sheet was also seen at the start and the end, with periods of lobe between 23 UT, DOY 286, and 18 UT, DOY 287. However, three intervals of plasma, with fluxes in both the sunwards and tailwards directions, were detected at the same time as CAAs were observed by DMSP/SSUSI, associated with excursions to  $|\theta| < 45^\circ$  (n). Plasma was also seen by C4 in the southern tail at these times (Figure 5), and the plasma characteristics were similar. The presence of fluxes in both the sunwards and tailwards directions, indicate that the plasma was trapped on closed field lines. During the second orbit, the magnetic field observed by the Magnetic Field Experiment (MGF) instrument (Kokubun et al., 1994), panel d,

matched closely the prediction by T96. However, during the first orbit, around the time Geotail was in the lobe the  $B_x$  component was elevated above the prediction (c) indicating an inflated magnetotail.

### 3. Discussion

The occurrence of CAAs filling the polar regions is frequent. We find that CAAs have a high probability of appearing if  $|\theta| < 45^\circ$  for an appreciable length of time (1–2 hr or more). During our period of study, CAAs were observed for approximately 30% of the time. Although polar cap arcs received attention in the past (e.g., Ismail et al., 1977), CAAs are too dim to have been detected by previous generations of global auroral imaging missions (e.g., Polar and IMAGE), so their importance has been overlooked. We find that CAAs are accompanied by dense plasma of energies from several eV to several 10s keV in regions of the magnetosphere (up to  $|Z| \approx 13 R_E$  in our observations) that would normally be occupied by the evacuated tail lobes. This implies that much of the previously open flux of the lobes has been closed and that the plasma sheet is encroaching on regions which would previously have been open lobes. In fact, below we will argue that the magnetosphere is almost entirely closed, that it is filled with plasma trapped from the solar wind, and that this acts as a source of plasma to produce auroral emissions across the polar regions.

Several mechanisms have been proposed by which plasma could enter the tail during NBZ conditions (Taylor et al., 2008), including inward diffusion at the flanks (e.g., Fujimoto et al., 1998, 2000; Terasawa et al., 1997) and lobe reconnection, either single (Shi et al., 2013) or double (Imber et al., 2006; Milan, Carter, Bower, et al., 2020; Øieroset et al., 2005). For instance, Shi et al. (2013) interpreted similar observations of plasma in the “open lobes” as an indication of direct ingress of solar wind plasma via single lobe reconnection. However, it seems unlikely that this plasma would reside in the near-Earth tail for long, as it would escape down the tail along the open field lines and be lost back to the solar wind, as occurs during periods of southwards IMF. Instead, we suggest that this plasma must be trapped on closed field lines. This interpretation is supported by the presence of a double loss-cone in the C4 electron pitch angle distributions: this suggests that the electrons have interacted with the atmosphere in both northern and southern hemispheres over several bounces. The presence of counter-streaming ions observed by C4 is also consistent with closed field lines and trapped plasma, as are the sunwards/tailwards fluxes observed by Geotail: if the magnetic field was open, only tailward fluxes would be expected. This trapped plasma is observed in both the northern and southern portions of the magnetotail, at  $Z \approx 8 R_E$  and  $Z \approx -13 R_E$ , simultaneously (see Figures 5 and 7). Assuming that the tail is roughly north-south symmetric, then this implies that the plasma sheet is at least of order  $30 R_E$  thick and a very large proportion of the magnetospheric flux is closed.

A means to produce closed magnetic flux during NBZ, simultaneously trapping solar wind plasma in the magnetotail to first produce a low-latitude boundary layer and then a cold, dense plasma sheet, is DLR (e.g., Cowley, 1981; Dungey, 1963; Imber et al., 2006; Øieroset et al., 2005, 2008; Song & Russell, 1992). Milan, Carter, Bower, et al. (2020) argued that DLR explains multiple aspects of the interaction: the capture and trapping of plasma, the four-cell ionospheric flow pattern, and the auroral evolution observed during the formation of HCAs and by extension CAAs (Milan et al., 2022). DLR also explains the necessity for near-zero clock angle,  $|\theta| < 45^\circ$ , for the appearance of HCAs (Bower, Milan, Paxton, & Anderson, 2022) and CAAs (this study). If DLR continues for long enough, the magnetosphere should close (almost) entirely and enter a mode of reverse convection (Milan et al., 2022; Siscoe et al., 2011; Song & Russell, 1992; Wang et al., 2023). As we argue below, we believe that the magnetosphere is indeed (almost) entirely closed when CAAs are observed, and that the cold, dense plasma sheet occupies the whole tail.

The plasma trapped by DLR acts as a source for precipitation to produce auroral emission at high latitudes. It might be imagined that if the whole tail is closed and filled with plasma, then blanket auroral emission would be observed over the whole polar regions. On the other hand, as the electron pitch angle distribution has empty loss cones (Figure 6f), the plasma should mirror above the ionosphere and not produce auroras, unless accelerated downwards. In fact, auroras are seen, but in the form of CAAs. As shown by Milan et al. (2022) and Q.-H. Zhang et al. (2020), CAAs are produced by inverted-V precipitation, electrons accelerated to energies of a few keV, at shears in the ionospheric convection flow. These shears are associated with converging electric field and Pederesen current in the ionosphere: an upwards electric field is generated above the ionosphere to accelerate electrons downwards to provide current continuity. Hence, the trapped plasma acts as a reservoir from which field-aligned currents can be supplied as required by flow shears. As indicated in Figure 3, although there are gaps between the CAAs (Figure 2f), weak inverted-Vs are observed everywhere, but produce emission too faint to be detected by

DMSP/SSUSI. Precipitating ions with energies of one to several keV are also observed in the ionosphere when CAAs are present (Milan et al., 2022), consistent with the trapped ions found in this study in the magnetotail and observed in the ionosphere (Figure 3). Whereas Carlson and Cowley (2005) proposed that weak polar cap arcs are produced by accelerated polar rain on open field lines, in our scenario trapped solar wind plasma on closed field lines is the more readily available source population.

So, how closed is the magnetosphere? The electron double loss-cone signature seen in this study is similar to the plasma characteristics seen by Fear et al. (2014) at high  $Z$  over a transpolar arc. In that case, the plasma was only observed by Cluster on closed field lines that mapped to the arc, and evacuated lobe was seen to either side, suggesting that the magnetosphere remained significantly open. In our case the plasma is observed for prolonged periods (sometimes many hours) wherever C4 is located in the tail and wherever it maps to in the polar ionosphere (Figure 2), whether that be close to a CAA (e.g., panel i) or in a gap between CAAs (e.g., panel f). This suggests that dim regions in the polar ionosphere do not necessarily imply open flux, but that plasma is trapped above the ionosphere and is not being accelerated downwards to produce significant auroras. We also note that the distributions of locations of C4 when CAAs are present (and plasma is seen in the tail), Figure 1b, and over the 15 days study period, Figure 1a, are not significantly different: there is no preferred location for C4 to see the trapped plasma. Also, as C4 maps to almost the dayside oval (Figures 2i and 2j) and CAAs are seen to extend all the way to the dayside oval (Figure 2e), we conclude that the magnetosphere does indeed close (almost) entirely. (We have repeatedly added the caveat “almost,” as Milan et al. (2022) suggested that once the magnetosphere is closed it is probable that single lobe reconnection can open flux, such that it may intermingle with the closed flux, as also suggested by Øieroset et al. (2008).) That the field is closed at high latitudes also explains why CAAs are generally seen in both hemispheres simultaneously (see Figure 2 and Milan et al., 2022), whereas other polar cap auroral phenomena are not always conjugate (e.g., Bower, Milan, Paxton, & Imber, 2022; Reidy et al., 2020).

As shown by Milan et al. (2022), when CAAs are observed, the large scale ionospheric flow pattern has reverse lobe convection cells, consistent with DLR (Reiff & Burch, 1985), though on smaller scales multiple flow shears are seen, which accelerate plasma to produce the auroral emissions. Wang et al. (2023) and Q.-H. Zhang et al. (2020) suggested that these flow shears are produced by Kelvin-Helmholtz instability (KHI) waves on the magnetospheric flanks propagating into the magnetotail. However, the cusp-aligned nature of the arcs shows that the flow shears are also cusp-aligned, which is not necessarily predicted by the KHI mechanism. Instead, Milan et al. (2022) proposed that the flow shears are excited by temporally- and spatially-varying lobe reconnection rates, which naturally explains why the flows and shears radiate from the cusp region. Dual-lobe reconnection explains the closure of magnetic flux and the trapping of solar wind plasma, it explains the “reverse” flow pattern observed in the ionosphere, it explains the structuring of the auroral precipitation into multiple arcs, and it also explains why the arcs are “cusp-aligned.”

DLR does not close the magnetosphere instantly, but progressively, first producing the HCA configuration before CAAs. Due to the poor cadence of the auroral observations it is difficult to determine how rapidly this occurs. We note that between 22 UT, DOY 285, and 08 UT, DOY 286, there were two brief swings of the clock angle to  $|\theta| < 45^\circ$ , but no CAAs were detected and open lobe was observed by C4 (see Figure 5). This suggests that there is a minimum duration of DLR of 1–2 hr for plasma to be trapped throughout the magnetosphere, consistent with the 1-hr delay to full-closure observed by Øieroset et al. (2008). This minimum will be related to the reconnection rate, that is the rate at which flux is closed, such that open lobe is replaced by closed flux containing trapped solar wind plasma. Detailed measurement of the rate of closure will be required to further understand this, perhaps facilitated by ionospheric convection measurements (e.g., Chisham et al., 2004, 2008). We contrast the 1–2 hr timescale observed for plasma to fill the tail, with the flank diffusion rates estimated by Fujimoto et al. (1998), which imply that diffusion would take many hours to achieve only limited filling.

As an aside, we note that the magnitude of the  $B_x$  component of the IMF was significant at times, for example,  $\approx 10$  nT during the first period of CAAs in Figure 4, and was near-zero at others, for example, the last period of CAAs in Figure 5. This suggests that  $B_x$  does not play a role in modulating the occurrence of (dual-) lobe reconnection and hence the occurrence of CAAs. This tallies with a lack of  $B_x$  control of the occurrence of HCAs reported by Bower, Milan, Paxton, and Anderson (2022).

Once DLR ceases the magnetosphere loses the trapped plasma and the polar cap reforms promptly, indicating the rapid opening of magnetic flux by magnetopause reconnection. This opening will occur most rapidly if the IMF is directed southwards and subsolar reconnection occurs, which will be accompanied by twin-cell convection in

the polar ionosphere. However, as noted by Milan et al. (2022), it will also occur if the IMF is directed northwards with  $|\theta| > 45^\circ$  as single lobe reconnection will open a closed magnetosphere. Hence, CAAs are only seen for  $|\theta| < 45^\circ$ .

Empirical magnetic field models, such as T96, do not reproduce a closed magnetosphere well, though closed NBZ magnetospheres are readily formed in simulations (e.g., Siscoe et al., 2011; Song et al., 1999; Wang et al., 2023). The magnetic field measurements made by C4/FGM and Geotail/MGF indicated that the  $B_X$  component was reduced when CAAs were present, with respect to when open lobe was observed. This indicates that the tail is somewhat deflated when it is closed (though it could also be in part because plasma pressure contributes to stress balance in the closed tail, rather than just magnetic pressure in the lobes). However, otherwise the field did not deviate markedly from the T96 predictions, indicating that if the magnetosphere is indeed closed, the magnetic structure near-Earth is not significantly modified, suggesting that the closed field lines stretch considerably further down-tail than the locations of C4 and Geotail. This is consistent with the observations of Øieroset et al. (2008), of a closed magnetotail extending far antisunward of the Earth, but in contradiction to simulations which suggest that a closed magnetotail might be less than  $20 R_E$  in length (Wang et al., 2023). On the other hand, Milan, Carter, and Hubert (2020) estimated that closed field lines associated with transpolar arcs could extend as far as  $X < -100 R_E$ . More work needs to be conducted in the distant magnetotail and with magnetospheric simulations to understand the magnetic topology of the closed magnetosphere.

#### 4. Conclusions

We have investigated a 15-day period during which Cluster and Geotail sampled the magnetotail. Observations of the auroras by DMSP/SSUSI indicates that CAAs were present in the high latitude polar regions whenever the IMF clock angle was small,  $|\theta| < 45^\circ$ , which during the study interval amounted to approximately 30% of the time. Simultaneous observations of ions and electrons by Cluster and Geotail show significant plasma densities ( $n_i \approx n_e \approx 1 \text{ cm}^{-3}$ ) in the tail during these intervals, even as far from the equatorial plane as  $|Z| \approx 13 R_E$ . This region of the magnetotail would normally be devoid of plasma, being occupied by the open flux of the magnetotail lobes. The presence of counter-streaming ions and double loss-cone electrons suggest, instead, that the plasma was trapped, that is, that the magnetic field was closed. This trapped plasma will provide a source for the CAA auroral emission, and as the auroral emission (and associated precipitation) covered the polar regions, we further suggest that the magnetosphere was almost entirely closed. Coxon et al. (2021) recently showed that hot plasma consistent with trapping on closed field lines is frequently seen at  $|Z| > 5 R_E$  during northward IMF; here we have shown that CAAs are the auroral signature of this closed flux, and that at such times the magnetosphere is likely (almost) entirely closed. We believe that this closure is achieved by DLR, as proposed by Milan, Carter, Bower, et al. (2020) and Milan et al. (2022). Our observations indicate that closure of the magnetosphere is a common occurrence.

#### Data Availability Statement

Data from the Cluster Ion Spectrometry (CIS) instrument, the Plasma Electron And Current Experiment (PEACE), and the Fluxgate Magnetometer (FGM) were accessed through the Cluster Science Archive (CSA, formerly Cluster Active Archive; Laakso et al., 2010) at <https://www.cosmos.esa.int/web/csa>, maintained by ESA/ESTEC. Geotail Magnetic Field Experiment (MGF) and Low Energy Particle (LEP) data were accessed through the DARTS Solar-Terrestrial Physics data portal (<https://www.darts.isas.jaxa.jp/stp/geotail/data.html>) maintained by ISAS/JAXA. The Defense Meteorological Satellite Program (DMSP) Special Sensor Ultraviolet Spectrographic Instrument (SSUSI) file type EDR-AUR data were obtained from JHU/APL (<http://ssusi.jhuapl.edu>, data version 0106, software version 7.0.0, calibration period version E0018). The DMSP SSI/4 particle detector data were obtained from JHU/APL ([http://sd-www.jhuapl.edu/Aurora/dataset\\_list.html](http://sd-www.jhuapl.edu/Aurora/dataset_list.html)), and processed using software provided (<http://sd-www.jhuapl.edu/Aurora/software/index.html>). Advanced Magnetosphere and Planetary Electrodynamics Response Experiment (AMPERE) data were obtained from JHU/APL (<https://ampere.jhuapl.edu/dataget/index.html>) and processed using software provided (<https://ampere.jhuapl.edu/>). The high resolution (1-min) OMNI data used in this study were obtained from the NASA Goddard Space Flight Center Space Physics Data Facility OMNIWeb portal ([https://omniweb.gsfc.nasa.gov/form/om\\_filt\\_min.html](https://omniweb.gsfc.nasa.gov/form/om_filt_min.html)).

### Acknowledgments

SEM and MKM were supported by the Science and Technology Facilities Council (STFC), UK, Grant ST/S000429/1. SEM and GEB were supported by the Natural Environment Research Council (NERC), UK, Grant NE/W006766/1. We are grateful to the Cluster CIS, PEACE, and FGM instrument teams for providing data. We acknowledge use of NASA/GSFC's Space Physics Data Facility's CDAWeb service (at <http://cdaweb.gsfc.nasa.gov>), and OMNI data, and the Cluster Science Archive (at <https://www.cosmos.esa.int/web/csa>), maintained by ESA/ESTEC. Geotail magnetic field and plasma data were provided by T. Nagai and Y. Saito through DARTS at the Institute of Space and Astronomical Science, JAXA, in Japan. The DMSP SSIJ/4 particle detectors were designed by Dave Hardy of AFRL.

### References

- Anderson, B., Takahashi, K., & Toth, B. (2000). Sensing global Birkeland currents with Iridium® engineering magnetometer data. *Geophysical Research Letters*, 27(24), 4045–4048. <https://doi.org/10.1029/2000GL000094>
- Balogh, A., Dunlop, M., Cowley, S., Southwood, D., Thomlinson, J., Glassmeier, K., et al. (1997). The cluster magnetic field investigation. *Space Science Reviews*, 79(1/2), 65–91. <https://doi.org/10.1023/A:1004970907748>
- Bogdanova, Y., Owen, C., Dunlop, M., Wild, J., Davies, J., Lahiff, A., et al. (2008). Formation of the low-latitude boundary layer and cusp under the northward IMF: Simultaneous observations by Cluster and Double Star. *Journal of Geophysical Research*, 113(A7), A07S07. <https://doi.org/10.1029/2007JA012762>
- Bower, G., Milan, S., Paxton, L., & Anderson, B. (2022). Occurrence statistics of horse collar aurora. *Journal of Geophysical Research: Space Physics*, 127(5), e2022JA030385. <https://doi.org/10.1029/2022JA030385>
- Bower, G., Milan, S., Paxton, L., & Imber, S. (2022). Transpolar arcs: Seasonal dependence identified by an automated detection algorithm. *Journal of Geophysical Research: Space Physics*, 127(1), e2021JA029743. <https://doi.org/10.1029/2021JA029743>
- Carlson, H., & Cowley, S. (2005). Accelerated polar rain electrons as the source of sun-aligned arcs in the polar cap during northward interplanetary magnetic field conditions. *Journal of Geophysical Research*, 110(A5), A05302. <https://doi.org/10.1029/2004ja010669>
- Carter, J., Milan, S., Fogg, A., Paxton, L., & Anderson, B. (2018). The association of high-latitude dayside aurora with NBZ field-aligned currents. *Journal of Geophysical Research: Space Physics*, 123(5), 3637–3645. <https://doi.org/10.1029/2017JA025082>
- Carter, J., Milan, S., Fogg, A., Sangha, H., Lester, M., Paxton, L., & Anderson, B. (2020). The evolution of long-duration cusp spot emission during lobe reconnection with respect to field-aligned currents. *Journal of Geophysical Research: Space Physics*, 125(7), e2020JA027922. <https://doi.org/10.1029/2020JA027922>
- Chisham, G., Freeman, M., Abel, G., Lam, M., Pinnock, M., Coleman, I., et al. (2008). Remote sensing of the spatial and temporal structure of magnetopause and magnetotail reconnection from the ionosphere. *Reviews of Geophysics*, 46(1), RG1004. <https://doi.org/10.1029/2007RG000223>
- Chisham, G., Freeman, M., Coleman, I., Pinnock, M., Hairston, M., Lester, M., & Sofko, G. (2004). Measuring the dayside reconnection rate during an interval of due northward interplanetary magnetic field. *Annales Geophysicae*, 22(12), 4243–4258. <https://doi.org/10.5194/angeo-22-4243-2004>
- Chisham, G., Lester, M., Milan, S. E., Freeman, M., Bristow, W., Grocott, A., et al. (2007). A decade of the Super Dual Auroral Radar Network (SuperDARN): Scientific achievements, new techniques and future directions. *Surveys in Geophysics*, 28(1), 33–109. <https://doi.org/10.1007/s10712-007-9017-8>
- Cowley, S. (1981). Magnetospheric and ionospheric flow and the interplanetary magnetic field. In *The physical basis of the ionosphere in the solar-terrestrial system*, AGARD-CP-295 (pp. 4-1–4-14).
- Cowley, S., & Lockwood, M. (1992). Excitation and decay of solar wind-driven flows in the magnetosphere-ionosphere system. *Annales Geophysicae*, 10, 103–115.
- Coxon, J., Fear, R., Reidy, J., Fryer, L., & Plank, J. (2021). Hot plasma in the magnetotail lobes shows characteristics consistent with closed field lines trapped in the lobes. *Journal of Geophysical Research: Space Physics*, 126(9), e2021JA029516. <https://doi.org/10.1029/2021JA029516>
- Coxon, J., Milan, S., & Anderson, B. (2018). A review of Birkeland current research using AMPERE. In *Electric currents in geospace and beyond* (pp. 257–278). <https://doi.org/10.1002/9781119324522.ch16>
- Cummock, J., Sharber, J., Heelis, R., Blomberg, L. G., Germany, G., Spann, J., & Coley, W. (2002). Interplanetary magnetic field control of theta aurora development. *Journal of Geophysical Research*, 107(A7), S1A–4. <https://doi.org/10.1029/2001JA009126>
- Dungey, J. (1961). Interplanetary magnetic field and the auroral zones. *Physical Review Letters*, 6(2), 47–48. <https://doi.org/10.1103/physrevlett.6.47>
- Dungey, J. (1963). The structure of the exosphere, or adventures in velocity space. In C. DeWitt, J. Hieblot, & A. Leveau (Eds.), *Geophysics, The Earth's Environment* (pp. 505–550). Gordon and Breach.
- Escoubert, C., Fehringer, M., & Goldstein, M. (2001). Introduction the cluster mission. *Annales Geophysicae*, 19(10/12), 1197–1200. <https://doi.org/10.5194/angeo-19-1197-2001>
- Fear, R. (2021). The northward IMF magnetosphere. In *Magnetospheres in the solar system* (pp. 293–309). <https://doi.org/10.1002/9781119815624.ch19>
- Fear, R., & Milan, S. (2012a). The IMF dependence of the local time of transpolar arcs: Implications for formation mechanism. *Journal of Geophysical Research*, 117(A3), A03213. <https://doi.org/10.1029/2011ja017209>
- Fear, R., & Milan, S. (2012b). Ionospheric flows relating to transpolar arc formation. *Journal of Geophysical Research*, 117(A9), A09230. <https://doi.org/10.1029/2012ja017830>
- Fear, R., Milan, S., Maggiolo, R., Fazakerley, A., Dandouras, I., & Mende, S. (2014). Direct observation of closed magnetic flux trapped in the high-latitude magnetosphere. *Science*, 346(6216), 1506–1510. <https://doi.org/10.1126/science.1257377>
- Frank, L., Craven, J., Burch, J., & Winningham, J. (1982). Polar views of the Earth's aurora with dynamics explorer. *Geophysical Research Letters*, 9(9), 1001–1004. <https://doi.org/10.1029/GL009i009p01001>
- Frey, H. (2007). Localized aurora beyond the auroral oval. *Reviews of Geophysics*, 45(1), RG1003. <https://doi.org/10.1029/2005RG000174>
- Frey, H., Mende, S., Immel, T., Fuselier, S., Clafin, E., Gérard, J.-C., & Hubert, B. (2002). Proton aurora in the cusp. *Journal of Geophysical Research*, 107(A7), SMP–2. <https://doi.org/10.1029/2001JA900161>
- Fryer, L., Fear, R., Coxon, J., & Gingell, I. (2021). Observations of closed magnetic flux embedded in the lobes during periods of northward IMF. *Journal of Geophysical Research: Space Physics*, 126(6), e2021JA029281. <https://doi.org/10.1029/2021JA029281>
- Fujimoto, M., Mukai, T., Matsuoka, A., Saito, Y., Hayakawa, H., Kokubun, S., & Lepping, R. (2000). Multi-point observations of cold-dense plasma sheet and its relation with tail-LLBL. *Advances in Space Research*, 25(7–8), 1607–1616. [https://doi.org/10.1016/S0273-1177\(99\)00674-2](https://doi.org/10.1016/S0273-1177(99)00674-2)
- Fujimoto, M., Terasawa, T., Mukai, T., Saito, Y., Yamamoto, T., & Kokubun, S. (1998). Plasma entry from the flanks of the near-Earth magnetotail: Geotail observations. *Journal of Geophysical Research*, 103(A3), 4391–4408. <https://doi.org/10.1029/97JA03340>
- Fuselier, S., Trattner, K., Petrinc, S., & Lavraud, B. (2012). Dayside magnetic topology at the Earth's magnetopause for northward IMF. *Journal of Geophysical Research*, 117(A8), A08235. <https://doi.org/10.1029/2012JA017852>
- Hardy, D. (1984). Precipitating electron and ion detectors (SSIJ/4) for the block 5D/flights 6-10 DMSP satellites: Calibration and data presentation. Rep. AFGL-TR-84-0317.
- Hasegawa, H., Fujimoto, M., Phan, T.-D., Reme, H., Balogh, A., Dunlop, M., et al. (2004). Transport of solar wind into Earth's magnetosphere through rolled-up Kelvin-Helmholtz vortices. *Nature*, 430(7001), 755–758. <https://doi.org/10.1038/nature02799>
- Hones, E., Jr., Craven, J., Frank, L., Evans, D., & Newell, P. (1989). The horse-collar aurora: A frequent pattern of the aurora in quiet times. *Geophysical Research Letters*, 16(1), 37–40. <https://doi.org/10.1029/GL016i001p00037>

- Hosokawa, K., Kullen, A., Milan, S., Reidy, J., Zou, Y., Frey, H., et al. (2020). Aurora in the polar cap: A review. *Space Science Reviews*, 216(1), 15. <https://doi.org/10.1007/s11214-020-0637-3>
- Hosokawa, K., Moen, J., Shiokawa, K., & Otsuka, Y. (2011). Motion of polar cap arcs. *Journal of Geophysical Research*, 116(A1), A01305. <https://doi.org/10.1029/2010JA015906>
- Huang, C.-S., Sofko, G., Koustov, A., Andre, D., Ruohoniemi, J., Greenwald, R., & Hairston, M. (2000). Evolution of ionospheric multicell convection during northward interplanetary magnetic field with  $|B_z/B_y| > 1$ . *Journal of Geophysical Research*, 105(A12), 27095–27107. <https://doi.org/10.1029/2000JA000163>
- Iijima, T., & Potemra, T. (1976). The amplitude distribution of field-aligned currents at northern high latitudes observed by Triad. *Journal of Geophysical Research*, 81(13), 2165–2174. <https://doi.org/10.1029/JA081i013p02165>
- Iijima, T., Potemra, T., Zanetti, L., & Bythrow, P. (1984). Large-scale Birkeland currents in the dayside polar region during strongly northward IMF: A new Birkeland current system. *Journal of Geophysical Research*, 89(A9), 7441–7452. <https://doi.org/10.1029/JA089iA09p07441>
- Imber, S., Milan, S., & Hubert, B. (2006). The auroral and ionospheric flow signatures of dual lobe reconnection. *Annales Geophysicae*, 24(11), 3115–3129. <https://doi.org/10.5194/angeo-24-3115-2006>
- Ismail, S., Wallis, D., & Cogger, L. (1977). Characteristics of polar cap Sun-aligned arcs. *Journal of Geophysical Research*, 82(29), 4741–4749. <https://doi.org/10.1029/JA082i029p04741>
- Johnstone, A., Alsop, C., Burge, S., Carter, P., Coates, A., Coker, A., et al. (1997). Peace: A plasma electron and current experiment. *Space Science Reviews*, 79(1/2), 351–398. <https://doi.org/10.1023/A:1004938001388>
- King, J., & Papitashvili, N. (2005). Solar wind spatial scales in and comparisons of hourly wind and ACE plasma and magnetic field data. *Journal of Geophysical Research*, 110(A2), A02104. <https://doi.org/10.1029/2004JA010649>
- Kokubun, S., Yamamoto, T., Acuña, M., Hayashi, K., Shiokawa, K., & Kawano, H. (1994). The GEOTAIL magnetic field experiment. *Journal of Geomagnetism and Geoelectricity*, 46(1), 7–21. <https://doi.org/10.5636/jgg.46.7>
- Kullen, A., Brittnacher, M., Cumnock, J., & Blomberg, L. (2002). Solar wind dependence of the occurrence and motion of polar auroral arcs: A statistical study. *Journal of Geophysical Research*, 107(A11), 13–21. <https://doi.org/10.1029/2002JA009245>
- Laakso, H., Perry, C., McCaffrey, S., Herment, D., Allen, A., Harvey, C., et al. (2010). *Cluster active archive: Overview*. Springer.
- Lockwood, M., & Cowley, S. (1992). Ionospheric convection and the substorm cycle. In *Proceedings of the international conference on substorms (ICS-1)* (pp. 99–109).
- Mailyan, B., Shi, Q., Kullen, A., Maggiolo, R., Zhang, Y., Fear, R., et al. (2015). Transpolar arc observation after solar wind entry into the high-latitude magnetosphere. *Journal of Geophysical Research: Space Physics*, 120(5), 3525–3534. <https://doi.org/10.1002/2014ja020912>
- Milan, S., Bower, G., Carter, J., Paxton, L., Anderson, B., & Hairston, M. (2022). Lobe reconnection and cusp-aligned auroral arcs. *Journal of Geophysical Research: Space Physics*, 127(6), e2021JA030089. <https://doi.org/10.1029/2021JA030089>
- Milan, S., Carter, J., Bower, G., Imber, S., Paxton, L., Anderson, B., et al. (2020). Dual-lobe reconnection and horse-collar auroras. *Journal of Geophysical Research: Space Physics*, 125(10), e2020JA028567. <https://doi.org/10.1029/2020JA028567>
- Milan, S., Carter, J., & Hubert, B. (2020). Probing the magnetic structure of a pair of transpolar arcs with a solar wind pressure step. *Journal of Geophysical Research: Space Physics*, 125(2), e2019JA027196. <https://doi.org/10.1029/2019ja027196>
- Milan, S., Carter, J., Sangha, H., Bower, G., & Anderson, B. (2021). Magnetospheric flux throughput in the Dungey cycle: Identification of convection state during 2010. *Journal of Geophysical Research: Space Physics*, 126(2), e2020JA028437. <https://doi.org/10.1029/2020JA028437>
- Milan, S., Cowley, S., Lester, M., Wright, D., Slavin, J., Fillingim, M., & Singer, H. (2004). Response of the magnetotail to changes in the open flux content of the magnetosphere. *Journal of Geophysical Research*, 109(A4), A04220. <https://doi.org/10.1029/2003JA010350>
- Milan, S., Hubert, B., & Grocott, A. (2005). Formation and motion of a transpolar arc in response to dayside and nightside reconnection. *Journal of Geophysical Research*, 110(A1), A01212. <https://doi.org/10.1029/2004JA010835>
- Milan, S., Lester, M., Cowley, S., & Brittnacher, M. (2000). Dayside convection and auroral morphology during an interval of northward interplanetary magnetic field. *Annales Geophysicae*, 18(4), 436–444. <https://doi.org/10.1007/s00585-000-0436-9>
- Milan, S., Lester, M., Cowley, S., Oksavik, K., Brittnacher, M., Greenwald, R., et al. (2003). Variations in the polar cap area during two substorm cycles. *Annales Geophysicae*, 21(5), 1121–1140. <https://doi.org/10.5194/angeo-21-1121-2003>
- Milan, S., Provan, G., & Hubert, B. (2007). Magnetic flux transport in the Dungey cycle: A survey of dayside and nightside reconnection rates. *Journal of Geophysical Research*, 112(A1), A01209. <https://doi.org/10.1029/2006JA011642>
- Mukai, T., Machida, S., Saito, Y., Hirahara, M., Terasawa, T., Kaya, N., et al. (1994). The low energy particle (LEP) experiment onboard the Geotail satellite. *Journal of Geomagnetism and Geoelectricity*, 46(8), 669–692. <https://doi.org/10.5636/jgg.46.669>
- Nishida, A. (1994). The GEOTAIL mission. *Wiley Online Library*, 21(25), 2871–2873. <https://doi.org/10.1029/94gl01223>
- Øieroset, M., Phan, T., Fairfield, D., Raeder, J., Gosling, J., Drake, J., & Lin, R. (2008). The existence and properties of the distant magnetotail during 32 hours of strongly northward interplanetary magnetic field. *Journal of Geophysical Research*, 113(A4), A04206. <https://doi.org/10.1029/2007JA012679>
- Øieroset, M., Raeder, J., Phan, T., Wing, S., McFadden, J., Li, W., et al. (2005). Global cooling and densification of the plasma sheet during an extended period of purely northward IMF on October 22–24, 2003. *Geophysical Research Letters*, 32(12), L12S07. <https://doi.org/10.1029/2004gl021523>
- Paxton, L., Meng, C.-I., Fountain, G., Ogorzalek, B., Darlington, E., Gary, S., et al. (1992). Special sensor ultraviolet spectrographic imager: An instrument description. In *Instrumentation for planetary and terrestrial atmospheric remote sensing* (Vol. 1745, pp. 2–15). <https://doi.org/10.1117/12.60595>
- Paxton, L., Schaefer, R., Zhang, Y., & Kil, H. (2017). Far ultraviolet instrument technology. *Journal of Geophysical Research: Space Physics*, 122(2), 2706–2733. <https://doi.org/10.1002/2016JA023578>
- Paxton, L., & Zhang, Y. (2016). Far ultraviolet imaging of the aurora. In *Space weather fundamentals* (pp. 213–244). CRC Press.
- Paxton, L., Zhang, Y., Kil, H., & Schaefer, R. (2021). Exploring the upper atmosphere: Using optical remote sensing. In *Upper atmosphere dynamics and energetics* (pp. 487–522). <https://doi.org/10.1002/9781119815631.ch23>
- Reidy, J., Fear, R., Whiter, D., Lanchester, B., Kavanagh, A., Price, D. J., et al. (2020). Multiscale observation of two polar cap arcs occurring on different magnetic field topologies. *Journal of Geophysical Research: Space Physics*, 125(8), e2019JA027611. <https://doi.org/10.1029/2019ja027611>
- Reiff, P., & Burch, J. (1985). IMF By-dependent plasma flow and Birkeland currents in the dayside magnetosphere: 2. A global model for northward and southward IMF. *Journal of Geophysical Research*, 90(A2), 1595–1609. <https://doi.org/10.1029/JA090iA02p01595>
- Rème, H., Bosqued, J., Sauvaud, J., Cros, A., Dandouras, J., Aoustin, C., et al. (1997). The cluster ion spectrometry (cis) experiment. In *The cluster and phoenix missions* (pp. 303–350). Springer. [https://doi.org/10.1007/978-94-011-5666-0\\_12](https://doi.org/10.1007/978-94-011-5666-0_12)
- Rich, F., & Hairston, M. (1994). Large-scale convection patterns observed by DMSP. *Journal of Geophysical Research*, 99(A3), 3827–3844. <https://doi.org/10.1029/93JA03296>



- Shi, Q., Zong, Q.-G., Fu, S., Dunlop, M., Pu, Z., Parks, G., et al. (2013). Solar wind entry into the high-latitude terrestrial magnetosphere during geomagnetically quiet times. *Nature Communications*, *4*(1), 1466. <https://doi.org/10.1038/ncomms2476>
- Siscoe, G., Farrugia, C., & Sandholt, P. (2011). Comparison between the two basic modes of magnetospheric convection. *Journal of Geophysical Research*, *116*(A5), A05210. <https://doi.org/10.1029/2010JA015842>
- Siscoe, G., & Huang, T. (1985). Polar cap inflation and deflation. *Journal of Geophysical Research*, *90*(A1), 543–547. <https://doi.org/10.1029/ja090ia01p00543>
- Song, P., DeZeeuw, D., Gombosi, T., Groth, C., & Powell, K. (1999). A numerical study of solar wind-magnetosphere interaction for northward interplanetary magnetic field. *Journal of Geophysical Research*, *104*(A12), 28361–28378. <https://doi.org/10.1029/1999JA900378>
- Song, P., & Russell, C. (1992). Model of the formation of the low-latitude boundary layer for strongly northward interplanetary magnetic field. *Journal of Geophysical Research*, *97*(A2), 1411–1420. <https://doi.org/10.1029/91JA02377>
- Taylor, M., Lavraud, B., Escoubet, C., Milan, S., Nykyri, K., Dunlop, M., et al. (2008). The plasma sheet and boundary layers under northward IMF: A multi-point and multi-instrument perspective. *Advances in Space Research*, *41*(10), 1619–1629. <https://doi.org/10.1016/j.asr.2007.10.013>
- Terasawa, T., Fujimoto, M., Mukai, T., Shinohara, I., Saito, Y., Yamamoto, T., et al. (1997). Solar wind control of density and temperature in the near-earth plasma sheet: Wind/geotail collaboration. *Geophysical Research Letters*, *24*(8), 935–938. <https://doi.org/10.1029/96GL04018>
- Tsyganenko, N. (1995). Modeling the Earth's magnetospheric magnetic field confined within a realistic magnetopause. *Journal of Geophysical Research*, *100*(A4), 5599–5612. <https://doi.org/10.1029/94JA03193>
- Wang, X.-Y., Zhang, Q.-H., Wang, C., Zhang, Y.-L., Tang, B.-B., Xing, Z.-Y., et al. (2023). Unusual shrinkage and reshaping of Earth's magnetosphere under a strong northward interplanetary magnetic field. *Communications Earth & Environment*, *4*(1), 31. <https://doi.org/10.1038/s43247-023-00700-0>
- Waters, C., Anderson, B., & Liou, K. (2001). Estimation of global field aligned currents using the Iridium® system magnetometer data. *Geophysical Research Letters*, *28*(11), 2165–2168. <https://doi.org/10.1029/2000GL012725>
- Zhang, Q.-H., Zhang, Y.-L., Wang, C., Lockwood, M., Yang, H.-G., Tang, B.-B., et al. (2020). Multiple transpolar auroral arcs reveal insight about coupling processes in the Earth's magnetotail. *Proceedings of the National Academy of Sciences*, *117*(28), 16193–16198. <https://doi.org/10.1073/pnas.2000614117>
- Zhang, Y., Paxton, L., Newell, P., & Meng, C.-I. (2009). Does the polar cap disappear under an extended strong northward IMF? *Journal of Atmospheric and Solar-Terrestrial Physics*, *71*(17–18), 2006–2012. <https://doi.org/10.1016/j.jastp.2009.09.005>
- Zhang, Y., Paxton, L., Zhang, Q.-H., & Xing, Z. (2016). Polar cap arcs: Sun-aligned or cusp-aligned? *Journal of Atmospheric and Solar-Terrestrial Physics*, *146*, 123–128. <https://doi.org/10.1016/j.jastp.2016.06.001>